



## Genomic insights and prognostic significance of novel biomarkers in pancreatic ductal adenocarcinoma: A comprehensive analysis

Yuling Chen<sup>a,1</sup>, Anle Huang<sup>b,1</sup>, Yuanjie Bi<sup>c</sup>, Wei Wei<sup>d</sup>, Yongsheng Huang<sup>c,\*\*</sup>,  
Yuanchun Ye<sup>c,e,f,\*</sup>

<sup>a</sup> Department of Rheumatology and Immunology, The Seventh Affiliated Hospital, Sun Yat-sen University, Shenzhen, Guangdong Province, China

<sup>b</sup> Department of Gastrointestinal Oncology Surgery, The First Affiliated Hospital of Xiamen University, School of Medicine, Xiamen University, Xiamen, Fujian, China, 361001

<sup>c</sup> School of Science, Shenzhen Campus of Sun Yat-Sen University, Shenzhen, 518107, China

<sup>d</sup> Department of Emergency, The Seventh Affiliated Hospital, Sun Yat-sen University, Shenzhen, Guangdong Province, China

<sup>e</sup> Shenzhen Bay Laboratory, Shenzhen, Guangdong Province, China

<sup>f</sup> Department of Hematology Oncology and Tumor Immunity, Benjamin Franklin Campus, Charité-Universitätsmedizin Berlin, Corporate Member of Freie Universität Berlin, Humboldt-Universität zu Berlin, Berlin, Germany

### ARTICLE INFO

#### Keywords:

Pancreatic ductal adenocarcinoma  
Prognostic signature  
RNA-seq analysis

### ABSTRACT

Pancreatic ductal adenocarcinoma (PDAC) is a highly prevalent digestive system malignancy, with a significant impact on public health, especially in the elderly population. The advent of the Human Genome Project has opened new avenues for precision medicine, allowing researchers to explore genetic markers and molecular targets for cancer diagnosis and treatment. Despite significant advances in genomic research, early diagnosis of pancreatic cancer remains elusive due to the lack of highly sensitive and specific markers. Therefore, there is a need for in-depth research to identify more precise and reliable diagnostic markers for pancreatic cancer. In this study, we utilized a combination of public databases from different sources to meticulously screen genes associated with prognosis in pancreatic cancer. We used gene differential analysis, univariate cox regression analysis, least absolute selection and shrinkage operator (LASSO) regression, and multivariate cox regression analysis to identify genes associated with prognosis. Subsequently, we constructed a scoring system, validated its validity using survival analysis and ROC analysis, and further confirmed its reliability by nomogram and decision curve analysis (DCA). We evaluated the diagnostic value of this scoring system for pancreatic cancer prognosis and validated the function of the genes using single cell data analysis. Our analysis identifies six genes, including GABRA3, IL20RB, CDK1, GPR87, TTYH3, and KCNA2, that were strongly associated with PDAC prognosis. Clinical prognostic models based on these genes showed strong predictive power not only in the training set but also in external datasets. Functional enrichment analysis revealed significant differences between high- and low-risk groups mainly in immune-related functions. Additionally, we explored the potential of the risk score as a marker for immunotherapy response and identified key factors within the tumor microenvironment. The single-cell RNA sequencing analysis further enriched our understanding of cell clusters and six hub genes expressions. This comprehensive investigation provides valuable insights into pancreatic PDAC and its intricate immune landscape. The identified genes and their functional significance underscore the importance of continued research into improving diagnosis and treatment strategies for PDAC.

### 1. Introduction

Pancreatic cancer ranks among the most prevalent digestive system

\* Corresponding author. School of Science, Sun Yat-Sen University, Shenzhen 518107, China.

\*\* Corresponding author.

E-mail addresses: [chenyuling@sysush.com](mailto:chenyuling@sysush.com), [chenyuling53@mail.sysu.edu.cn](mailto:chenyuling53@mail.sysu.edu.cn) (Y. Chen), [huang\\_anle@163.com](mailto:huang_anle@163.com) (A. Huang), [biyj@mail.sysu.edu.cn](mailto:biyj@mail.sysu.edu.cn) (Y. Bi), [weiw68@mail.sysu.edu.cn](mailto:weiw68@mail.sysu.edu.cn) (W. Wei), [huangysh59@mail.sysu.edu.cn](mailto:huangysh59@mail.sysu.edu.cn) (Y. Huang), [yeyuanchun1357@163.com](mailto:yeyuanchun1357@163.com), [Yuanchun.ye@charite.de](mailto:Yuanchun.ye@charite.de) (Y. Ye).

<sup>1</sup> Yuling Chen and Anle Huang contributed equally to this work.

tumors, predominantly afflicting the elderly, typically manifesting after the age of 65 [1]. According to cancer statistics in 2022, pancreatic

survival analysis, and further substantiated its reliability through nomogram and decision curve analysis (DCA). We then proceeded to

Abbreviation		
AUC	area under the ROC	logFC
BF	biological processes	log (fold change)
CC	cellular components	LUAD
CDKs	cyclin-dependent kinases	lung adenocarcinoma
DCA	decision curve analysis	LUSC
GABA	$\gamma$ -aminobutyric acid	lung squamous cell carcinoma
GEO	gene expression omnibus	MF
GO	gene ontology	and molecular functions
GSEA	gene set enrichment analysis	OS
GSVA	gene set variation analysis	overall survival
HGP	Human Genome Project	PACA-AU
HR	hazard ratios	pancreatic cancer Australia cohere
ICGC	International Cancer Genome Consortium	PACA-CA
IQR	interquartile range	pancreatic cancer Canada cohere
KNN	K-nearest neighbor	PCA
LASSO	least absolute selection and shrinkage operator	principal component analysis
		PDAC
		pancreatic ductal adenocarcinoma
		ROC
		receiver operating characteristic
		scRNA-seq
		single-cell RNA sequencing
		SKCM
		skin cutaneous melanoma
		STAD
		stomach adenocarcinoma
		TIDE
		Tumor Immune Dysfunction and Exclusion
		tSNE
		t-distributed stochastic neighbor embedding
		UCEC
		uterine corpus endometrial carcinoma
		UMAP
		uniform manifold approximation and projection

cancer ranks as the 10th most common cancer in males and the 8th most common cancer in females concerning malignancies within the United States, while simultaneously occupying the grim rank of the 4th leading cause of cancer-related fatalities [2]. Alarming, a study spanning 28 European nations forecasts that pancreatic cancer may outpace breast cancer, emerging as the third most fatal cancer by 2025 [3]. However, this menacing disease is notorious for eluding early diagnosis, with over 80 % of patients receiving the grim news of an unresectable tumor at a late stage. Moreover, even with surgical resection, the 5-year survival rate plummets to a disheartening 8.9 % in the United States [4]. Pancreatic ductal adenocarcinoma (PDAC) accounts for 90 % of all pancreatic cancer cases [5]. Therefore, it remains imperative to intensify research efforts geared towards the identification and development of biomarkers that can revolutionize early detection strategies for PDAC.

The completion of the Human Genome Project (HGP) has ushered in a new era of medical technologies, including gene testing, and has paved the way for precision medicine driven by extensive data analysis. This progress has brought about innovative approaches to the diagnosis and treatment of tumors, such as gene diagnostics and gene therapy [6]. Through large-scale genomic data collection and analysis, researchers can identify specific genetic variants and molecular markers associated with PDAC, which enable more accurate diagnosis, even at an early stage [7]. Noteworthy genomic research has identified that common mutation sites in PDAC include KRAS, TP53, PALB2, and SMAD4 [8,9]. However, challenges persist in the realm of early PDAC diagnosis, primarily due to the lack of highly sensitive and specific markers. This deficiency poses a significant hurdle to early detection, particularly since PDAC often progresses silently without overt symptoms. The predictive accuracy of existing markers falls short, leading to the potential for misdiagnosis or the failure to detect the disease in its initial phases [10]. Given these critical limitations, there is an urgent need to uncover more precise and reliable diagnostic markers for PDAC, which is essential to enhance the chances of timely intervention and improved outcomes for patients.

In this study, we systematically utilized a variety of public databases from diverse sources to meticulously screen for genes associated with prognosis of PDAC by using gene differential analysis, univariate cox regression analysis, least absolute selection and shrinkage operator (LASSO) regression, and multivariate cox regression analysis. Subsequently, we constructed a scoring system, rigorously validated it using

evaluate the diagnostic value of our scoring system in predicting the prognosis of PDAC and substantiated its functionality through single-cell RNA sequencing (scRNA-seq) analysis. We firmly believe that our research will make a significant contribution to the robust analysis of prognostic indicators at the genetic level in PDAC and provide effective biomarkers for its diagnosis and prognosis.

## 2. Method

### 2.1. Data collection and analysis

TCGA-GETx PDAC transcriptome, genome, and clinical information were downloaded from the UCSC Xena platform (<https://xena.ucsc.edu/>) [11], while pancreatic cancer Australia cohere (PACA-AU) and Canada cohere (PACA-CA) transcriptome and clinical information were obtained from the International Cancer Genome Consortium (ICGC) website (<https://dcc.icgc.org/>) [12]. Pancreatic cancer microarray data (GSE57495, GSE85916) were downloaded from the GEO database (<https://www.ncbi.nlm.nih.gov/geo/>) [13]. The sample selection criteria were as follows: (1) exclusion of patients with non-pancreatic ductal adenocarcinoma; (2) exclusion of patients with incomplete prognostic information and a survival time of less than 30 days; (3) exclusion of patients with concomitant malignant tumors in other sites or those who received chemotherapy and radiotherapy. Detailed clinical information is presented in Table 1. The analytical workflow is illustrated in Fig. 1.

### 2.2. Screening of prognostic-related differentially expressed genes and construction of risk score

The tumor and normal tissues of TCGA and GETx datasets were grouped, and differentially expressed coding genes were extracted using the DESeq2 package [14] with a threshold of  $|\logFC| > 1$  & adjust  $p$  value  $< 0.05$ . Prognostic-related differentially expressed genes were screened using survival analysis with a threshold of  $p < 0.05$ . The TCGA dataset was divided into a training set and a testing set in a 1:1 ratio. Univariate cox regression analysis, LASSO regression, and multivariate cox regression analysis were conducted based on the clinical information and expression profile information to identify the prognostic-related differentially expressed coding genes. Then, the risk score was calculated based on gene expression values and HR values using the formula:

**Table 1**  
The clinical characteristics of the patients used in the paper.

	TCGA			<i>p</i>	ICGC		GEO	
	All	Test set	Train set		PACA-AU	PACA-CA	GSE57495	GSE85916
n	129	64	65		55	105	63	79
Gender female (%)	60(46.5)	27(42.2)	33(50.8)	0.423	26(47.3)	49(47.1)	–	–
age (Median [IQR])	65.82 [56.82, 73.35]	64.81 [55.53, 72.35]	67.33 [57.49, 73.35]	0.214	68.50 [57.25, 75.75]	64.00 [57.00, 73.00]	–	–
T_stage (%)				0.032				
T1	4 (3.1)	4 (6.2)	0 (0.0)	–	4 (7.4)	–	–	–
T2	13 (10.1)	8 (12.5)	5 (7.7)	–	48 (88.9)	–	–	–
T3	109 (84.5)	49 (76.6)	60 (92.3)	–	1 (1.9)	–	–	–
T4	3 (2.3)	3 (4.7)	0 (0.0)	–	1 (1.9)	–	–	–
M_stage (%)				0.604				
M0	62 (48.1)	31 (48.4)	31 (47.7)	–	1 (1.9)	–	–	–
M1	4 (3.1)	1 (1.6)	3 (4.6)	–	3 (5.6)	–	–	–
MX	63 (48.8)	32 (50.0)	31 (47.7)	–	50 (92.6)	–	–	–
N_stage (%)				0.365				
N0	33 (25.6)	19 (29.7)	14 (21.5)	–	15 (27.8)	–	–	–
N1	95 (73.6)	45 (70.3)	50 (76.9)	–	38 (70.4)	–	–	–
NX	1 (0.8)	0 (0.0)	1 (1.5)	–	1 (1.9)	–	–	–
Stage (%)				0.146				
1	10 (7.8)	7 (10.9)	3 (4.6)	–	–	8(7.7)	13(20.6)	–
2	111 (86.0)	53 (82.8)	58 (89.2)	–	–	92(88.5)	50(79.4)	–
3	3 (2.3)	3 (4.7)	0 (0.0)	–	–	3(2.9)	–	–
4	4 (3.1)	1 (1.6)	3 (4.6)	–	–	1(1.0)	–	–
x	1 (0.8)	0 (0.0)	1 (1.5)	–	–	–	–	–
Survival time (Median [IQR])	1.28 [0.78, 1.82]	1.32 [0.78, 1.94]	1.28 [0.80, 1.68]	0.36	1.16 [0.71, 2.07]	1.67 [0.81, 3.46]	1.76 [1.13, 2.53]	1.50 [0.91, 2.63]

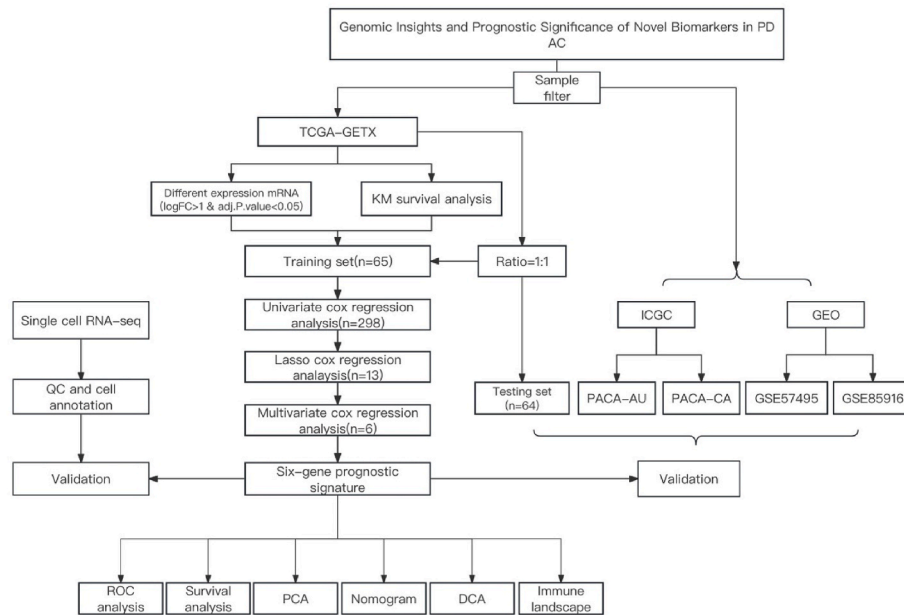


**Fig. 1.** Flow chart of the paper.

$$\text{Risk score} = \sum_{i=1}^N HRf_i * geneG_i.$$

### 2.3. Prognostic model performance validation

The prognostic risk scores calculated were used to divide the datasets (TCGA training set, testing set, ICGC and GEO datasets) into high-risk and low-risk groups based on the median risk score. Survival analysis was used to predict the overall survival (OS) between the two groups. The area under the time-dependent ROC curve (AUC) was used to quantify risk score model to predict the OS at 1-, 2-, and 3-year time point. Principal component analysis (PCA) was conducted on the samples to visualize the distribution of individual samples within these high and low-risk groups.

A multivariate cox regression model, including both risk scores and risk groups, was constructed and visualized using a nomogram. The model's performance was validated through calibration curves, and clinical benefits were evaluated using decision curve analysis (DCA).

### 2.4. Functional enrichment analysis

To clarify the potential biological functions of the high-risk and low-risk groups, we performed gene ontology (GO) enrichment analysis, including biological processes (BF), cellular components (CC), and molecular functions (MF), as well as gene set enrichment analysis (GSEA). An adjusted *p* value < 0.05 was set as the threshold for significance.

## 2.5. Analysis of immune cell infiltration

To evaluate the predictive capacity of the scoring system concerning the tumor immune microenvironment, we utilized ESTIMATE algorithms [15] to calculate the ratio of immune cells to stromal cells in each sample. We also assessed the proportion of tumor-infiltrating immune cells using algorithms including ssGSEA [16], and xCELL [17].

Furthermore, in order to assess the immune therapy response in different risk groups, we employed the algorithms from the TIDE website (<http://tide.dfci.harvard.edu>) [18]. TIDE stands for Tumor Immune Dysfunction and Exclusion. The TIDE score for each tumor samples can serve as a surrogate biomarker to predict response to immune checkpoint blockade, including anti-PD1 and anti-CTLA4. Additionally, we also estimated the activity of 13 immune mediated functions [19] using GSVA, the reference file sees Table S1.

## 2.6. scRNA-seq data analysis

To further explore the role of six genes in PDAC, the scRNA-seq data obtained from National Genomics Data Center (<https://ngdc.cncb.ac.cn/>, NO: CRA001160) [20]. The "Seurat" package [21,22] was used for scRNA-seq analysis. The standard Seurat pipeline, including normalization, feature selection, and dimensional reduction with principal component analysis (PCA), t-distributed stochastic neighbor embedding (tSNE), and uniform manifold approximation and projection (UMAP), was used to construct a K-nearest neighbor (KNN) graph after dimensional reduction. We filtered out low-quality cells based on two criteria: (1) genes expressed less than 200 or greater than 2500; (2) mitochondrial-associated genes expressed more than 10 %. The top 3000 variable genes were detected using the "vst" selection method. PCA was then performed, and the top 20 principal components were used for dimensional reduction using Seurat's built-in PCA, tSNE, or UMAP.

Cell types were annotated based on expression of known markers: EPCAM, KRT8, CFTR, MMP7, CDH5, PLVAP, VWF, CLDN5 (endocrine cell), LUM, DCN, COL1A1, SPARC, ACTA2, TAGLN (fibroblast), AIF1, CD68, HLA-DRA (macrophage), CD3D, CD3E, CD3G (T cell), MS4A1, CD79A, CD79B (B cell).

## 2.7. Statistical analysis

All statistical tests were considered significant if the  $p$  value was less than 0.05. R version 4.1.2 (R Foundation for Statistical Computing, Vienna, Austria) and RStudio were used to perform all statistical analyses [23,24]. Package used in software included: caret [25], survival [26], glmnet [27], survminer [28], forestplot [29], rms [30], cowplot [31], ggrrisk [32], ggsci [33], scatterplot3d [34], survivalROC [35], enrichplot [36], clusterProfiler [37], regplot [38], ggDCA [39], ggplot2 [40], org.Hs.eg.db [41], IOBR [42], GSVA [43].

## 3. Results

### 3.1. Clinical feature used in the study

After sample filtration, a total of 129 PDAC patients from TCGA, 55 from PACA-AU, 105 from PACA-CA, 63 from GSE57495, and 79 from GSE85916 were included for subsequent analysis. Among the 129 patients from TCGA, 65 were randomly assigned to the training set, while 64 were designated for the testing set, and no statistically significant differences were observed in the grouping analysis. The results indicated that the distribution of gender in PDAC patients ranged from 46.5 % to 47.3 % (female), the mean age varied from 64y to 68.5y, and the average survival time spanned from 1.16 to 1.76 years, and most patients (79.4 %–89.2 %) were in stage 2, with minimal variation among data from different sources (Table 1).

### 3.2. Prognosis-related genes and the construction of models

Firstly, a total of 7212 differentially expressed genes were identified between the tumor group and the normal group. Among them, 743 mRNA showed a significant correlation with patient clinical prognosis and were further screened through univariate cox regression analysis, LASSO regression, and multivariate cox regression analysis using the training set. Ultimately, 6 mRNA including GABRA3, IL20RB, CDK1, GPR87, TTYH3, and KCNA2, were selected for constructing the tumor prognosis model (Table S2). Notably, the expression levels of 6 genes exhibited a significant correlation with PDAC survival prognosis (Fig. 2). Among them, high expression of GABRA3, TTYH3, and KCNA2 was associated with a favorable prognosis in PDAC, indicating a protective role. Conversely, high expression of IL20RB, CDK1, and GPR87 suggested a higher likelihood of these genes acting as oncogenes, and their increased expression was correlated with an adverse prognosis.

### 3.3. Clinical prognostic model evaluation and validation

A risk score model was constructed based on the expression values of six genes and hazard ratios (HR) obtained from multivariate cox regression, and its clinical utility was assessed through survival analysis and ROC analysis. This model exhibited robust predictive capabilities, performing well not only in the training set but also in the test set of the same cohort. Furthermore, its predictive performance extended to external cohorts, including the ICGC datasets (PACA-AU, PACA-CA) and the GEO datasets (GSE85916, GSE57495), where high-risk score groups showed poorer clinical outcomes, with  $p$ -values all less than 0.05 (Fig. 3). Additionally, based on ROC analysis, in the validation set, the risk score demonstrated good prognostic value for 1-year OS in pancreatic cancer, with AUC values ranging from 0.6 to 0.748 (Fig. 4). Moreover, the risk score plot constructed from multivariate cox regression indicated that most patients with a clinical outcome of death were predominantly in the high-risk score group. And the heatmap showed differential expression of the six hub genes among different risk score groups (Fig. 5). Among these genes, patients with high expression of KCNA, TTYH3, and low expression of GPR87, CDK1, IL20RB, GABRA3 consistently exhibited a better prognosis in the majority of the datasets. This aligns with the survival analysis findings presented in Fig. 2.

As evident from the three-dimensional PCA plots (Fig. 6A), the risk group effectively differentiate between various samples and likely account for approximately 65 % of the variability. Furthermore, a multivariate cox regression model that included age, gender, stage, risk score, and risk group was developed and visualized using a nomogram (Fig. 6B). Within this model, high-risk group, higher risk scores, and advanced N stage were identified as independent prognostic factors for 1-, 2-, 3-years OS in pancreatic cancer. The model's performance was assessed through calibration curve analysis, yielding a C-index of 0.751 (Fig. 6C). The prognostic benefit of the model was confirmed through diagnostic decision curve analysis (DCA), demonstrating that both model 1, which included risk score, and model 2, which included both risk group and risk score, provided greater utility than the baseline model (Fig. 6D).

### 3.4. Functional enrichment analysis

To comprehensively assess the effectiveness of the risk score system in pancreatic cancer, we conducted differential analysis and functional enrichment by stratifying the PAAD cohort into high-risk and low-risk groups based on the median scores of each sample. Our observations from both GO analysis and GSEA analysis revealed significant distinctions between these two groups, mainly in immune cell functions, including antigen binding, B-cell receptor signaling pathway, immune globulin complex pathway, etc. These findings indicated that the novel scoring system could serve as an effective tool for assessing immune-related functions in pancreatic cancer (Fig. 7).

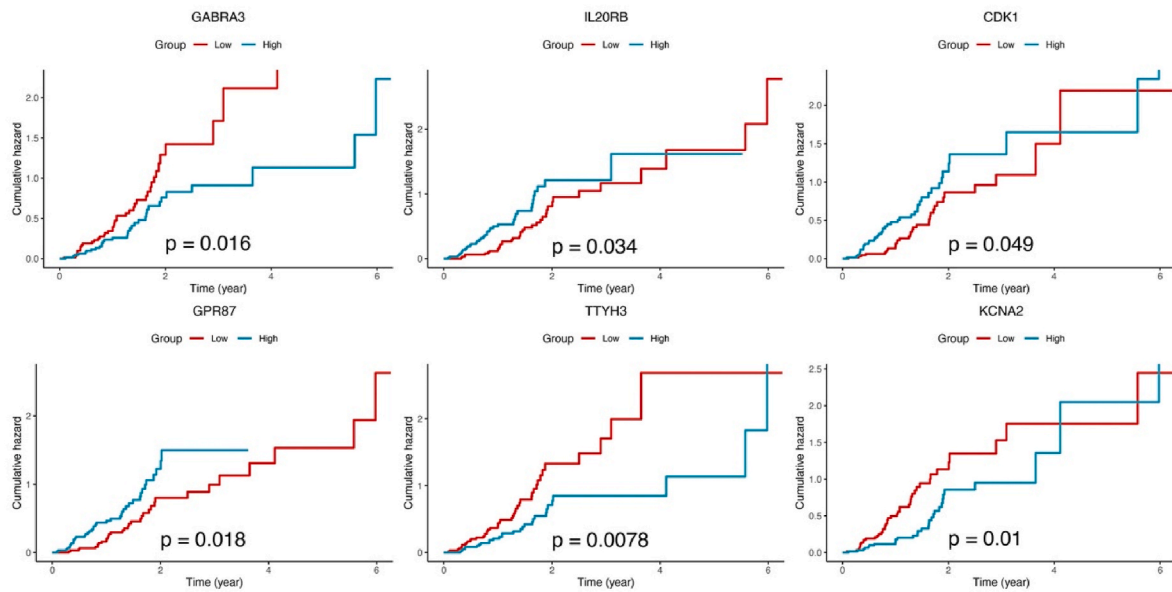


**Fig. 2.** Survival analysis of six hub gene in TCGA. Survival analysis of (A) GABRA3, (B) IL20RB, (C) CDK1, (D) GPR87, (E) TTYH3, and (F) KCNA2 in TCGA database. The red line represents samples with low gene expression, while the cyan line represents samples with high gene expression.

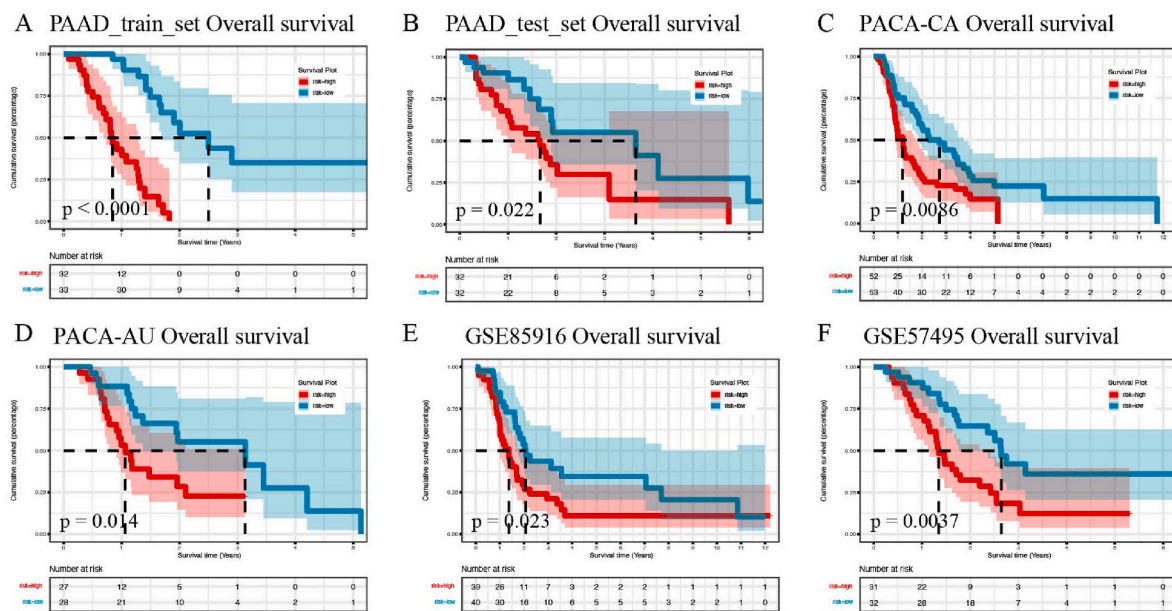


**Fig. 3.** Testing and validating the OS predictive performance of the risk score. The performance of the risk score in six independent datasets, including A: TCGA-Training set, B: TCGA-Testing set, C: PACA-CA, D: PACA-AU, E: GSE85916; and F: GSE57495. The red line represents samples with high-risk score, while the cyan line represents samples with low-risk score.

### 3.5. Immune cell infiltration

By applying algorithmic analysis of the tumor immune microenvironment, we expanded our study to examine the variations in immune cell infiltration between the high-risk and low-risk groups. We observed notable distinctions in central memory CD4 T cells, effector memory CD4/CD8 T cells, immature B cells, and natural killer cells (Fig. 8A), as well as variations in immune scores and stroma scores (Fig. 8B and C).

Regarding the response to immunotherapy, a noteworthy distinction in TIDE scores emerges between the high-risk and low-risk groups. This suggests that the risk score could potentially serve as one of the markers for identifying immunotherapy, as well as for uncovering immune dysfunction. Additionally, it might provide insights into the presence of

Merk18, MDSC, and CD8 cells within the tumor microenvironment. Moreover, it signified a positive response to T cell co-inhibition, T cell co-stimulation and IFNG treatment (Fig. 8D and E).

### 3.6. scRNA-seq profiling, clustering, and gene expression

After preprocessing the scRNA-seq data according to the stringent quality control criteria mentioned earlier, we included a total of 41,986 cancer cells in the analysis (Fig. S1). Employing PCA, tSNE, and UMAP classification methods, we categorized all cells into nine clusters, including ductal cells, fibroblasts, macrophages, endothelial cells, T cells, B cells, and other cell types (Fig. S2, Fig. 9A). The distribution of the six hub genes across these nine cell clusters reveals that CDK1 was

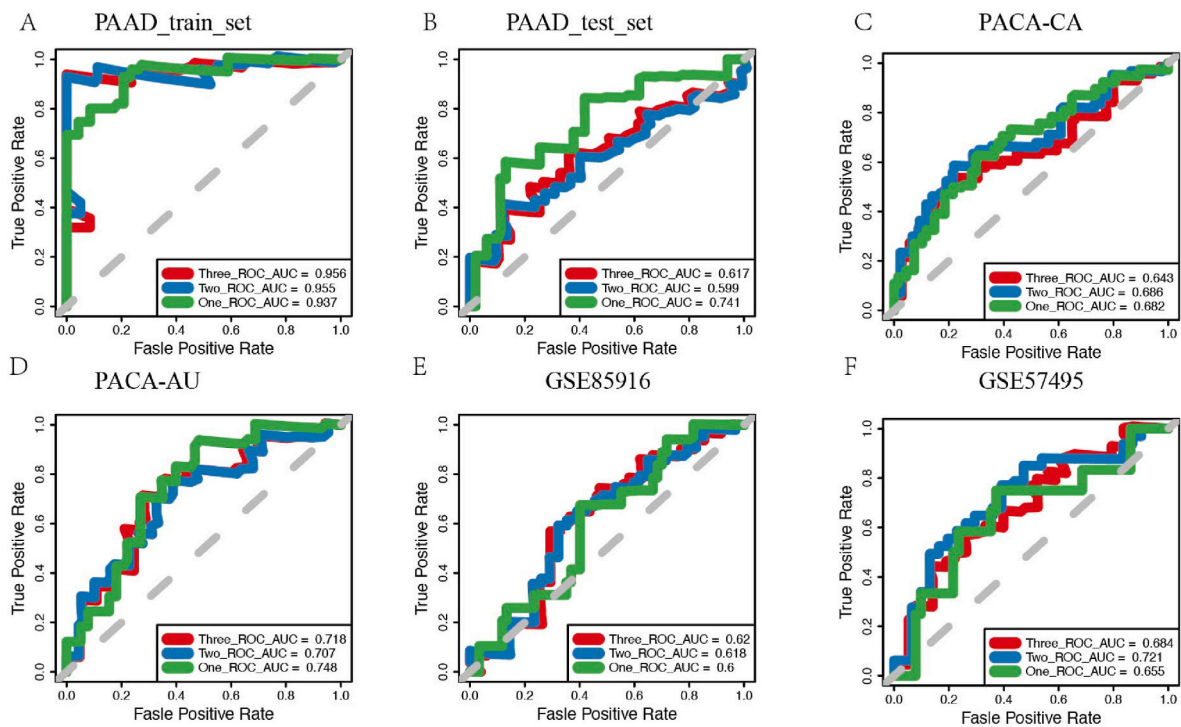


**Fig. 4.** Performing time-dependent ROC curve analysis for 1-year, 2-year, and 3-year OS. The risk score model for OS at 1-year, 2-year, and 3-year in datasets A: TCGA-Training set, B: TCGA-Testing set, C: PACA-CA, D: PACA-AU, E: GSE85916; F: GSE57495. AUC: area under the curve, ROC: receiver operating characteristic curve, OS: overall survival.

predominantly expressed in tumor cells, TTYH3 was mainly expressed in macrophages and tumor cells, while the remaining genes exhibited lower expression levels across other cell types (Fig. 9B and C).

#### 4. Discussion

Currently, numerous studies have focused on the identification of prognostic genes and predictive models for pancreatic cancer [44–47]. Our research results contribute significantly to enhancing our understanding of PDAC diagnosis and prognosis. The cohorts from various database sources show similar clinical characteristics, with pancreatic cancer being more prevalent in men and tending to affect older individuals. It's worth noting that there were more patients in stage 2, which could be attributed to the fact that the samples were primarily derived from surgical patients, that might influence our results. The identification of six prognostic genes and the development of a risk score model represent substantial contributions to this field. The model demonstrates robust predictive capabilities and has been validated across multiple external datasets, highlighting its potential clinical utility.

The six genes identified in our study, including GABRA3, IL20RB, CDK1, GPR87, TTYH3, and KCNA2. GABRA3, typically expressed in neuronal tissues, is a subunit of the cell surface receptor known as the  $\gamma$ -aminobutyric acid (GABA) type A receptor, which functions as a chloride channel. The expression of GABRA3 can influence the proliferation, migration, and invasion of pancreatic cancer cells [48] and breast cancer cells [49], designating it as one of the prognosis-related genes. However, it's worth noting that, at the single-cell level, we did not observe significant variations in the expression of this gene among different type of cells.

IL20RB, encoding the  $\beta$  subunit of the interleukin-20 receptor and forming a heterodimeric cytokine receptor with IL20RA or IL22RA1, has been associated with various human malignancies, including clear cell renal cell carcinoma, colorectal adenocarcinoma, and breast cancer [50–52]. Meanwhile, IL20RB has been associated with the prognosis of

PDAC [53], and the study have reported a negative correlation between its expression and that of PDL1, which could be used as an immunotherapeutic target [54]. In our study, we observed expression of this gene at the single-cell level and appeared to be higher in tumor cells. However, further in-depth research is required to fully understand its functionality.

CDK1, one of the cyclin-dependent kinases (CDKs) and the only essential CDK to drive the mammalian cell cycle [55], plays a role in both promoting and inhibiting tumor processes through substrate phosphorylation [56]. High expression of CDK1 in PDAC was associated with short survival [57]. Our study also confirmed that CDK1 is highly expressed in a small proportion of pancreatic ductal cells.

GPR87, known as G protein-coupled receptor 87, is newly deorphanized lysophosphatidic acid receptor G protein-coupled receptors [58]. It is upregulated in various malignancies and is vital to the proliferation and survival of tumor cells [59]. The expression of GPR87 is increased in pancreatic cancer contributing proliferation, angiogenesis, and increased resistance to gemcitabine-induced apoptosis and tumorigenicity [60].

TTYH3 belongs to tweety family of genes family encoding large conductance chloride (maxi-Cl<sup>-</sup>) channels [61,62]. TTYH3 was overexpressed and was correlation with the infiltration of TAMs, Treg infiltration T cell exhaustion and worse immunotherapy response in lung cancer tissues [63]. TTYH3 facilitated cellular migration and regulated expression of epithelial-mesenchymal transition-related protein by increasing calcium influx and intracellular chloride concentration in hepatocellular carcinoma [64].

KCNA2 is Potassium Voltage-Gated Channel Subfamily A Member 2, mainly expressed in the brain and the central nervous system [65,66]. A meta-analysis study showed that KCNA2, KCNA3, and KCNA5 as the predominant expressed KCNA family genes in skin cutaneous melanoma (SKCM), uterine corpus endometrial carcinoma (UCEC), stomach adenocarcinoma (STAD), lung adenocarcinoma (LUAD), and lung squamous cell carcinoma (LUSC); KCNA3 expression was related to prognosis in SKCM, LUAD, and LUSC and KCNA5 expression was related

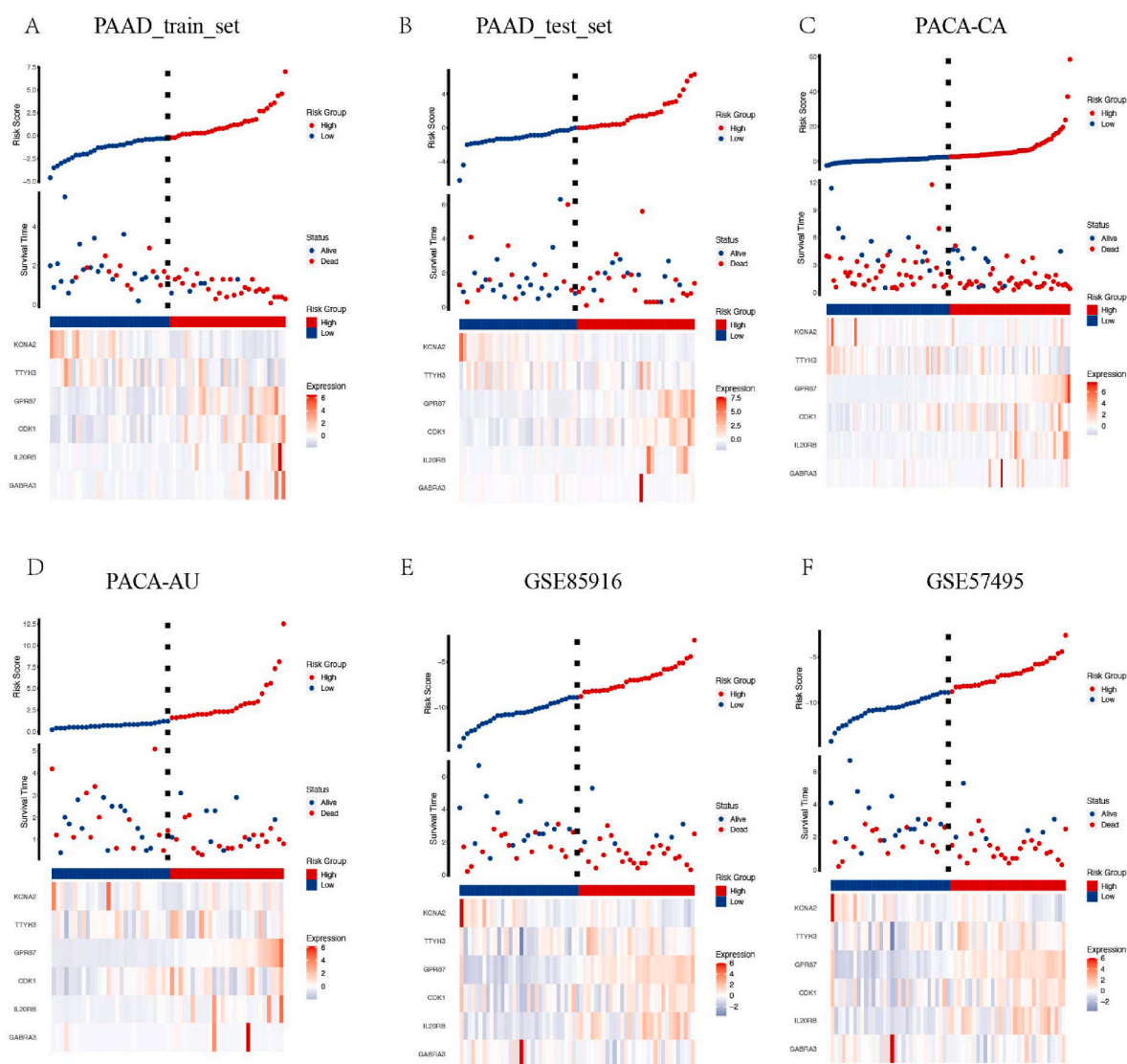


**Fig. 5.** Risk score plot based on multivariate cox regression. Risk curves and scatter plots display the risk score and outcome status of each sample in each database, including A: TCGA-Training set, B: TCGA-Testing set, C: PACA-CA, D: PACA-AU, E: GSE85916; F: GSE57495. The heatmap illustrates the expression levels of 6 genes in the high-risk and low-risk groups.

to prognosis in STAD, while *KCNA2* expression was notably correlated with patients' survival in cancers [67]. However, the survival analyses and the gene expression heat map in our study suggested that high expression of *KCNA2* in pancreatic cancer patients was linked to a better prognosis. This intriguing observation warrants further investigation and experimental confirmation in the future.

The use of a single gene to predict the prognosis of PDAC is indeed limited, which is why current studies often opt for multi-gene constructed models to predict tumor prognosis. Given that most pancreatic cancer patients have a survival period of only 1–2 years, early identification of patients with poor prognosis is of paramount importance. As illustrated in Fig. 3 (Survival Analysis) and Fig. 4 (Time-dependent ROC), our developed model showed a substantial difference in survival prediction, particularly within the 1 to 2-year range, across various external datasets. These findings underscore the diagnostic and prognostic potential of our model for early identification and risk assessment in PDAC patients.

Our study constructed a scoring system that observed differences in immune cell function between risk groups. There is an intricate relationship between immune cell function and PDAC, which often creates an immunosuppressive microenvironment that hinders immune cell

activity. Immune cells such as T cells and natural killer cells play a crucial role in tumor surveillance and eradication. It is critical to understand the functional dynamics of these cells in the context of PDAC [68,69]. Immunotherapy stands as a beacon of hope in the quest to treat PDAC. Emerging strategies, including checkpoint inhibitors, hold substantial promise in ongoing clinical trials. Nevertheless, formidable therapeutic challenges persist, primarily rooted in PDAC's immunosuppressive microenvironment [70–72]. Accurately predicting and evaluating immunotherapy responses is paramount. Our scoring system plays a pivotal role in forecasting the efficacy of tumor immunotherapy, particularly with regards to T cell and IFN treatment. This progress marks a significant stride toward more effective PDAC therapies, offering renewed optimism for patients and clinicians.

In summary, our study provides a comprehensive exploration of prognostic-related genes and risk score models in PDAC. We identified six key genes—*GABRA3*, *IL20RB*, *CDK1*, *GPR87*, *TTYH3*, and *KCNA2*—that are important for PDAC prognosis. The strong predictive power of our risk score model was validated in different datasets, demonstrating its clinical potential to stratify patients and inform treatment decisions. Furthermore, our findings reveal the critical role of these genes in immune cell function and their relevance to PDAC immunotherapy. This

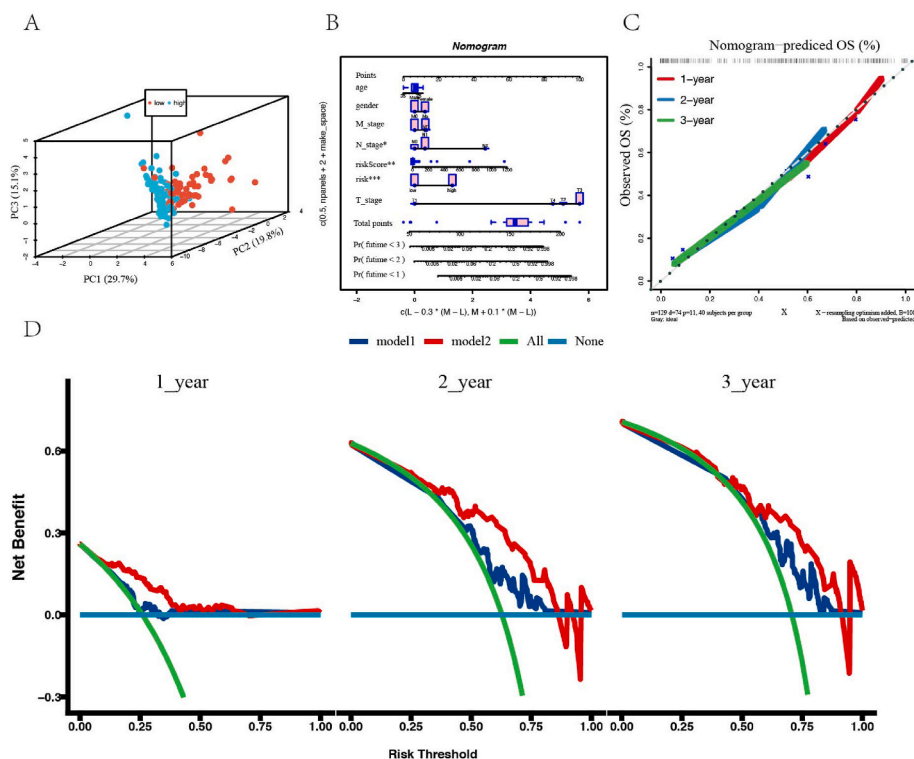


**Fig. 6.** Clinical prognostic model evaluation and validation. A.3D-PCA was conducted to visualize the distribution of individual samples within these high and low-risk groups. B. The nomogram showed the multivariate cox regression model constructed, including both risk scores and risk groups. C. Calibration curves confirm the predictive performance of the model for 1-, 2-, and 3-year OS. D. Decision curve analysis (DCA) was used to evaluate the clinical advantages of different models at 1-year, 2-year, and 3-year, including model1 with risk score and model2 with both risk score and risk group.

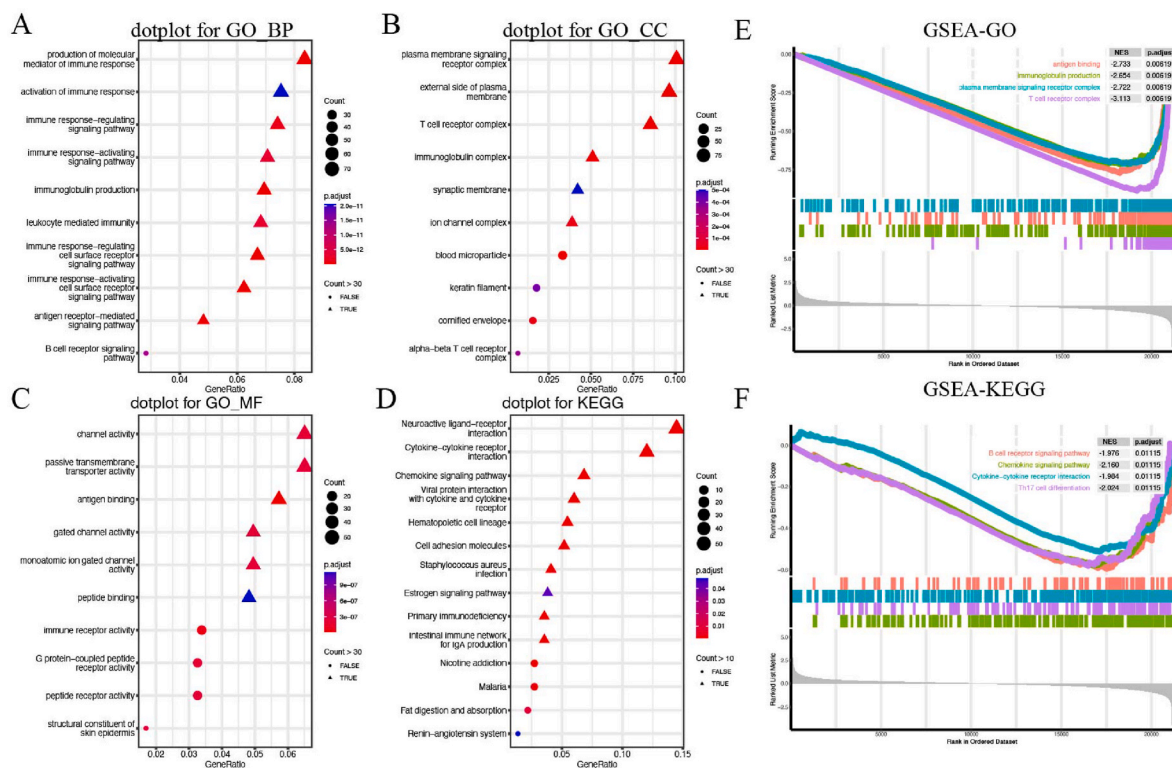


**Fig. 7.** Function enrichment analysis of risk score model. The top 10 terms in Biological Process (BP) (A), Cellular Component (CC) (B), and Molecular Function (MF) (C) categories from GO enrichment analysis. The top 15 terms in pathways from KEGG enrichment analysis (D). A multi-GSEA plot displaying the principal enrichment pathways in GO (E) and in KEGG (F).

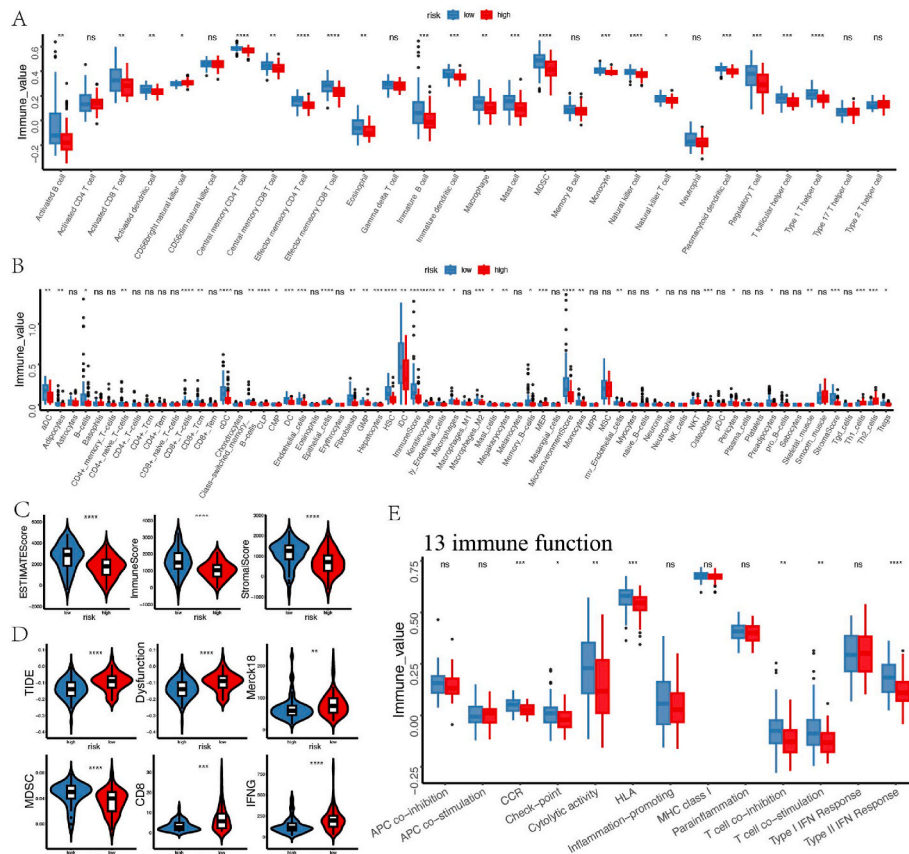


**Fig. 8.** Analysis of immune characteristics of high-risk and low-risk samples. The enrichment levels of different types of immune cells in the high-risk and low-risk groups, assessed using ssGSEA (A), xCell (B), and ESTIMATE (C) methods. The response to immunotherapy in different risk groups using TIDE score (D) and differences in 13 immune cells mediated functions between high-risk and low-risk groups (E).

knowledge provides valuable insights into enhancing the effectiveness of immunotherapeutic interventions against this challenging cancer. Essentially, our research helps improve diagnosis, prognostic assessment, and treatment strategies for PDAC, bringing hope for better outcomes and quality of life for affected individuals. Future studies should delve more deeply into the functional mechanisms of these genes and explore their therapeutic implications. PDAC research remains a dynamic field with great promise.

Although our study gained valuable insights, certain limitations should be acknowledged. First, although our risk score model showed good predictive power in different datasets, further validation in a larger and more diverse patient population is needed. Secondly, our analysis is mainly based on bioinformatics data, and the expression levels of the identified genes need to be experimentally verified in pancreatic cancer tissues or cells using techniques such as real-time PCR and Western blot analysis. Furthermore, our study focused on the prognostic impact of the identified genes without in-depth investigation of their functional mechanisms. Future studies should explore the potential biological processes by which these genes influence PDAC progression. Finally, while our study provides insights into immune cell function and immunotherapy, the actual clinical application of our findings requires further investigation and validation.

**Author contributions**

YYC, HYS put forward the conception, designed the study. CYL supervised the project and wrote the manuscript. YYC, BYJ, WW performed the analysis and prepared the figures and tables. HAL prepared the figures and revised the manuscript. All authors interpreted the experimental data, reviewed the manuscript, and approved the final

version.

**Funding**

This study was supported by Open Fund of Key Laboratory of Integrated Oncology and Intelligent Medicine of Zhejiang Province.

**Declarations**

None.

**Ethics approval and consent to participate**

None.

**Consent for publication**

Not applicable.

**Availability of data and materials**

The datasets used in the current study are publicly available data from UCSC Xena platform (<https://xena.ucsc.edu/>), ICGC website (<https://dcc.icgc.org/>), GEO (<https://www.ncbi.nlm.nih.gov/geo/>), and National Genomics Data Center (<https://ngdc.cncb.ac.cn/>). Further inquiries can be obtained directly from the corresponding author in a reasonable request.

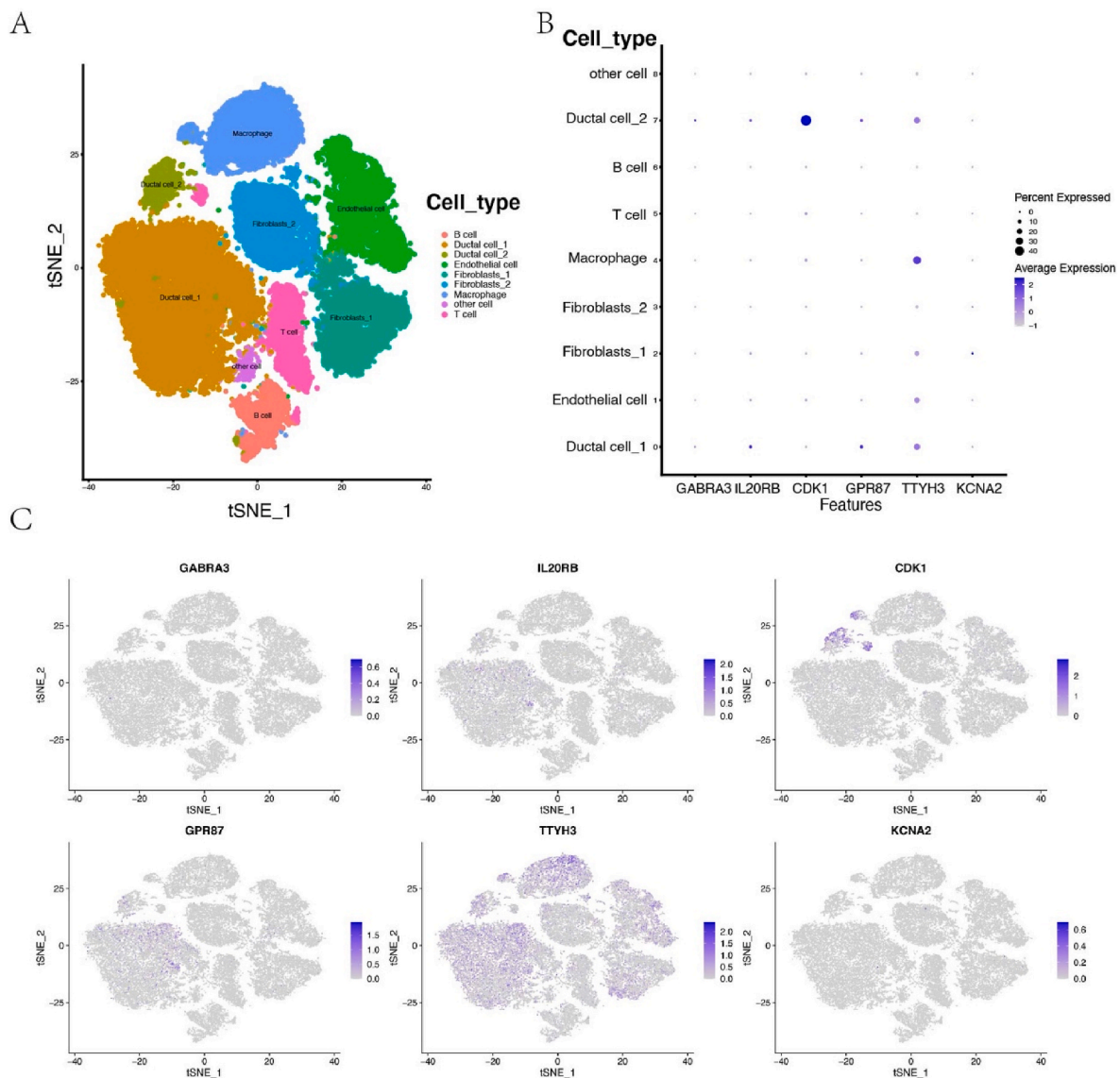


**Fig. 9.** Analysis of six hub genes at the single-cell level. A. The tSNE plot displays 9 distinct cell clusters with well-defined boundaries. B. Depicts the distribution of the 6 hub genes across various cell clusters. C. The tSNE plot illustrates the distribution of the 6 hub genes within the 9 cell clusters.

#### Declaration of competing interest

All authors declare no competing interests.

#### Data availability

Data will be made available on request.

#### Acknowledgements

We would like to thank those authors who shared their datasets on the UCSC Xena, ICGC, GEO, and NGDC databases.

#### Appendix A. Supplementary data

Supplementary data to this article can be found online at <https://doi.org/10.1016/j.bbrep.2023.101580>.

#### References

- [1] S. Gaddam, Y. Abboud, J. Oh, et al., Incidence of pancreatic cancer by age and sex in the US, 2000-2018, *JAMA*. Nov 326 (20) (23 2021) 2075–2077, <https://doi.org/10.1001/jama.2021.18859>.
- [2] R.L. Siegel, K.D. Miller, H.E. Fuchs, A. Jemal, Cancer statistics, *CA Cancer J Clin*. Jan 72 (1) (2022) 7–33, <https://doi.org/10.3322/caac.21708>, 2022.
- [3] J. Ferlay, C. Partensky, F. Bray, More deaths from pancreatic cancer than breast cancer in the EU by 2017, *Acta Oncol* 55 (9–10) (Sep-Oct 2016) 1158–1160, <https://doi.org/10.1080/0284186X.2016.1197419>.
- [4] C. Allemani, T. Matsuda, V. Di Carlo, et al., Global surveillance of trends in cancer survival 2000-14 (CONCORD-3): analysis of individual records for 37 513 025 patients diagnosed with one of 18 cancers from 322 population-based registries in 71 countries, *Lancet* 391 (10125) (Mar 17 2018) 1023–1075, [https://doi.org/10.1016/S0140-6736\(17\)33326-3](https://doi.org/10.1016/S0140-6736(17)33326-3).
- [5] J. Taieb, R. Abdallah, How I treat pancreatic cancer, *ESMO Open* 4 (Suppl 2) (Aug 2020), e000818, <https://doi.org/10.1136/esmoopen-2020-000818>.
- [6] C. Gonzaga-Jauregui, J.R. Lupski, R.A. Gibbs, Human genome sequencing in health and disease, *Annu. Rev. Med.* 63 (2012) 35–61, <https://doi.org/10.1146/annurev-med-051010-162644>.
- [7] T. Tanjo, Y. Kawai, K. Tokunaga, O. Ogasawara, M. Nagasaki, Practical guide for managing large-scale human genome data in research, *J Hum Genet.* Jan 66 (1) (2021) 39–52, <https://doi.org/10.1038/s10038-020-00862-1>.
- [8] H.F. Hu, Z. Ye, Y. Qin, et al., Mutations in key driver genes of pancreatic cancer: molecularly targeted therapies and other clinical implications, *Acta Pharmacol Sin.* Nov 42 (11) (2021) 1725–1741, <https://doi.org/10.1038/s41401-020-00584-2>.

- [9] O. Ge, A. Huang, X. Wang, Y. Chen, Y. Ye, L. Schomburg, PALB2 upregulation is associated with a poor prognosis in pancreatic ductal adenocarcinoma, *Oncol Lett.* Mar 21 (3) (2021) 224, <https://doi.org/10.3892/ol.2021.12485>.
- [10] G. Gheorghis, S. Bungau, M. Ilie, et al., Early diagnosis of pancreatic cancer: the key for survival, *Diagnostics* 10 (11) (Oct 24 2020), <https://doi.org/10.3390/diagnostics10110869>.
- [11] W.J. Kent, C.W. Sugnet, T.S. Furey, et al., The human genome browser at UCSC, *Genome Res.* Jun 12 (6) (2002) 996–1006, <https://doi.org/10.1101/gr.229102>.
- [12] J. Zhang, R. Bajari, D. Andric, et al., The international cancer genome Consortium data portal, *Nat Biotechnol.* Apr 37 (4) (2019) 367–369, <https://doi.org/10.1038/s41587-019-0055-9>.
- [13] R. Edgar, M. Domrachev, A.E. Lash, Gene Expression Omnibus: NCBI gene expression and hybridization array data repository, *Nucleic Acids Res.* Jan 1 30 (1) (2002) 207–210, <https://doi.org/10.1093/nar/30.1.207>.
- [14] M.I. Love, W. Huber, S. Anders, Moderated estimation of fold change and dispersion for RNA-seq data with DESeq2, *Genome Biol.* 15 (12) (2014) 550, <https://doi.org/10.1186/s13059-014-0550-8>.
- [15] K. Yoshihara, M. Shahmoradgolji, E. Martinez, et al., Inferring tumour purity and stromal and immune cell admixture from expression data, *Nat. Commun.* 4 (2013) 2612, <https://doi.org/10.1038/ncomms3612>.
- [16] D.A. Barbie, P. Tamayo, J.S. Boehm, et al., Systematic RNA interference reveals that oncogenic KRAS-driven cancers require TBK1, *Nature* 462 (7269) (Nov 5 2009) 108–112, <https://doi.org/10.1038/nature08460>.
- [17] D. Aran, Z. Hu, A.J. Butte, xCell: digitally portraying the tissue cellular heterogeneity landscape, *Genome Biol.* 18 (1) (Nov 15 2017) 220, <https://doi.org/10.1186/s13059-017-1349-1>.
- [18] J. Fu, K. Li, W. Zhang, et al., Large-scale public data reuse to model immunotherapy response and resistance, *Genome Med.* 12 (1) (Feb 26 2020) 21, <https://doi.org/10.1186/s13073-020-0721-z>.
- [19] M.S. Rooney, S.A. Shukla, C.J. Wu, G. Getz, N. Hacohen, Molecular and genetic properties of tumors associated with local immune cytolytic activity, *Cell* 160 (1–2) (Jan 15 2015) 48–61, <https://doi.org/10.1016/j.cell.2014.12.033>.
- [20] J. Peng, B.F. Sun, C.Y. Chen, et al., Single-cell RNA-seq highlights intra-tumoral heterogeneity and malignant progression in pancreatic ductal adenocarcinoma, *Cell Res.* Sep 29 (9) (2019) 725–738, <https://doi.org/10.1038/s41422-019-0195-y>.
- [21] Y. Hao, S. Hao, E. Andersen-Nissen, et al., Integrated analysis of multimodal single-cell data, *Cell* 184 (13) (Jun 24 2021) 3573–3587 e29, <https://doi.org/10.1016/j.cell.2021.04.048>.
- [22] T. Stuart, A. Butler, P. Hoffman, et al., Comprehensive integration of single-cell data, *Cell* 177 (7) (Jun 13 2019) 1888–1902 e21, <https://doi.org/10.1016/j.cell.2019.05.031>.
- [23] R.C.R. Team, A Language and Environment for Statistical Computing, 2020.
- [24] R. Team, RStudio, Integrated Development Environment for R, 2019.
- [25] M. Kuhn, Building predictive models in R using the caret package, *J. Stat. Software* 28 (5) (2008) 1–26, <https://doi.org/10.18637/jss.v028.i05>.
- [26] T.M. Therneau, A Package for Survival Analysis in {R}, 2020.
- [27] Ja.H. Friedman, Trevor and Tibshirani, robert. Regularization paths for generalized linear models via coordinate descent, *J. Stat. Software* 33 (2010) 1–22.
- [28] A. Kassambara, Survminer: Drawing Survival Curves Using 'ggplot2', 2016.
- [29] M.L.T. Gordon, Forestplot: Advanced Forest Plot Using, 'grid' Graphics, 2023.
- [30] E.H.J. Frank, Rms: Regression Modeling Strategies, 2023.
- [31] C.O. Wilke, Cowplot: Streamlined Plot Theme and Plot Annotations for, ggplot2, 2020.
- [32] JZaZ. Jin, Ggrisk: Risk Score Plot for Cox Regression, 2021.
- [33] N. Xiao, Ggsci: Scientific Journal and Sci-Fi Themed Color Palettes for, ggplot2, 2023.
- [34] U. Ligges, M. Maechler, scatterplot3d - an R package for visualizing multivariate data, *J. Stat. Software* 8 (11) (2003) 1–20, <https://doi.org/10.18637/jss.v008.i11>.
- [35] Saha-Chaudhuri PjhapbP, survivalROC: Time-dependent ROC Curve Estimation from Censored Survival Data, 2022.
- [36] G. Yu, Enrichplot: Visualization of Functional Enrichment Result, 2023, <https://doi.org/10.18129/B9.bioc.enrichplot>.
- [37] G. Yu, L.G. Wang, Y. Han, Q.Y. He, clusterProfiler: an R package for comparing biological themes among gene clusters, *OMICS.* May 16 (5) (2012) 284–287, <https://doi.org/10.1089/omi.2011.0118>.
- [38] Marshall) R. regplot, Enhanced Regression Nomogram Plot, 2020.
- [39] JZaZ. Jin, ggDCA: Calculate and Plot Decision Curve, 2023.
- [40] H. Wickham, ggplot2: Elegant Graphics for Data Analysis, 2016.
- [41] M. Carlson, org.Hs.eg.db: Genome Wide Annotation for Human, 2023.
- [42] D. Zeng, Z. Ye, R. Shen, et al., IOBR: multi-omics immuno-oncology biological research to decode tumor microenvironment and signatures, *Front. Immunol.* 12 (2021), 687975, <https://doi.org/10.3389/fimmu.2021.687975>.
- [43] S. Hanzelmann, R. Castelo, J. Guinney, GSEA: gene set variation analysis for microarray and RNA-seq data, *BMC Bioinf.* 14 (Jan 16 2013) 7, <https://doi.org/10.1186/1471-2105-14-7>.
- [44] K. Chen, Q. Wang, X. Liu, X. Tian, A. Dong, Y. Yang, Immune profiling and prognostic model of pancreatic cancer using quantitative pathology and single-cell RNA sequencing, *J. Transl. Med.* 21 (1) (Mar 21 2023) 210, <https://doi.org/10.1186/s12967-023-04051-4>.
- [45] K. Chen, X. Liu, W. Liu, F. Wang, X. Tian, Y. Yang, Development and validation of prognostic and diagnostic model for pancreatic ductal adenocarcinoma based on scRNA-seq and bulk-seq datasets, *Hum. Mol. Genet.* 31 (10) (May 19 2022) 1705–1719, <https://doi.org/10.1093/hmg/ddab343>.
- [46] G.G. Sharma, Y. Okada, D. Von Hoff, A. Goel, Non-coding RNA biomarkers in pancreatic ductal adenocarcinoma, *Semin. Cancer Biol.* 75 (Oct 2021) 153–168, <https://doi.org/10.1016/j.semcancer.2020.10.001>.
- [47] A.A. Tesfaye, A.S. Azmi, P.A. Philip, miRNA and gene expression in pancreatic ductal adenocarcinoma, *Am J Pathol.* Jan 189 (1) (2019) 58–70, <https://doi.org/10.1016/j.ajpath.2018.10.005>.
- [48] M. Long, M. Zhan, S. Xu, et al., miR-92b-3p acts as a tumor suppressor by targeting Gabra3 in pancreatic cancer, *Mol. Cancer* 16 (1) (Oct 27 2017) 167, <https://doi.org/10.1186/s12943-017-0723-7>.
- [49] K. Gumireddy, A. Li, A.V. Kossenkov, et al., The mRNA-edited form of GABRA3 suppresses GABRA3-mediated Akt activation and breast cancer metastasis, *Nat. Commun.* 7 (Feb 12 2016), 10715, <https://doi.org/10.1038/ncomms10715>.
- [50] H. Guo, S. Jiang, H. Sun, et al., Identification of IL20RB as a novel prognostic and therapeutic biomarker in clear cell renal cell carcinoma, *Dis. Markers* 2022 (2022), 9443407, <https://doi.org/10.1155/2022/9443407>.
- [51] Y. Zhang, Y. Liu, Y. Xu, Interleukin-24 regulates T cell activity in patients with colorectal adenocarcinoma, *Front. Oncol.* 9 (2019) 1401, <https://doi.org/10.3389/fonc.2019.01401>.
- [52] K. Omarini, S. Bettelli, C. Caprera, et al., Clinical and molecular predictors of long-term response in HER2 positive metastatic breast cancer patients, *Cancer Biol. Ther.* 19 (10) (2018) 879–886, <https://doi.org/10.1080/15384047.2018.1480287>.
- [53] W. Wang, L. Yan, X. Guan, et al., Identification of an immune-related signature for predicting prognosis in patients with pancreatic ductal adenocarcinoma, *Front. Oncol.* 10 (2020), 618215, <https://doi.org/10.3389/fonc.2020.618215>.
- [54] S.W. Lu, H.C. Pan, Y.H. Hsu, et al., IL-20 antagonist suppresses PD-L1 expression and prolongs survival in pancreatic cancer models, *Nat. Commun.* 11 (1) (Sep 14 2020) 4611, <https://doi.org/10.1038/s41467-020-18244-8>.
- [55] D. Santamaria, C. Barriere, A. Cerqueira, et al., Cdk1 is sufficient to drive the mammalian cell cycle, *Nature* 448 (7155) (Aug 16 2007) 811–815, <https://doi.org/10.1038/nature06046>.
- [56] Q. Wang, A.M. Bode, T. Zhang, Targeting CDK1 in cancer: mechanisms and implications, *npj Precis. Oncol.* 7 (1) (Jun 13 2023) 58, <https://doi.org/10.1038/s41698-023-00407-7>.
- [57] J. Piao, L. Zhu, J. Sun, et al., High expression of CDK1 and BUB1 predicts poor prognosis of pancreatic ductal adenocarcinoma, *Gene* 701 (Jun 15 2019) 15–22, <https://doi.org/10.1016/j.gene.2019.02.081>.
- [58] K. Tabata, K. Baba, A. Shiraishi, M. Ito, N. Fujita, The orphan GPCR GPR87 was deorphanized and shown to be a lysophosphatidic acid receptor, *Biochem. Biophys. Res. Commun.* 363 (3) (Nov 23 2007) 861–866, <https://doi.org/10.1016/j.bbrc.2007.09.063>.
- [59] S. Glatt, D. Halbauer, S. Heindl, et al., hGPR87 contributes to viability of human tumor cells, *Int. J. Cancer* 122 (9) (May 1 2008) 2008–2016, <https://doi.org/10.1002/ijc.23349>.
- [60] L. Wang, W. Zhou, Y. Zhong, et al., Overexpression of G protein-coupled receptor GPR87 promotes pancreatic cancer aggressiveness and activates NF-kappaB signaling pathway, *Mol. Cancer* 16 (1) (Mar 14 2017) 61, <https://doi.org/10.1186/s12943-017-0627-6>.
- [61] M. Suzuki, A. Mizuno, A novel human Cl(-) channel family related to Drosophila flightless locus, *J. Biol. Chem.* 279 (21) (May 21 2004) 22461–22468, <https://doi.org/10.1074/jbc.M313813200>.
- [62] F.K. Rae, J.D. Hooper, H.J. Eyre, G.R. Sutherland, D.L. Nicol, J.A. Clements, TTYH2, a human homologue of the Drosophila melanogaster gene tweety, is located on 17q24 and upregulated in renal cell carcinoma, *Genomics* 77 (3) (Oct 2001) 200–207, <https://doi.org/10.1006/geno.2001.6629>.
- [63] Z. Wei, X. Zeng, Y. Lei, et al., TTYH3, a potential prognosis biomarker associated with immune infiltration and immunotherapy response in lung cancer, *Int Immunopharmacol.* Sep 110 (2022), 108999, <https://doi.org/10.1016/j.intimp.2022.108999>.
- [64] Y. Wang, Y. Xie, B. Dong, et al., The TTYH3/MK5 positive Feedback loop regulates tumor progression via GSK3-beta/beta-catenin signaling in FCC, *Int. J. Biol. Sci.* 18 (10) (2022) 4053–4070, <https://doi.org/10.7150/ijbs.73009>.
- [65] J.S. Trimmer, Subcellular localization of K+ channels in mammalian brain neurons: remarkable precision in the midst of extraordinary complexity, *Neuron.* Jan 85 (2) (21 2015) 238–256, <https://doi.org/10.1016/j.neuron.2014.12.042>.
- [66] H. Vacher, D.P. Mohapatra, J.S. Trimmer, Localization and targeting of voltage-dependent ion channels in mammalian central neurons, *Physiol Rev.* Oct 88 (4) (2008) 1407–1447, <https://doi.org/10.1152/physrev.00002.2008>.
- [67] B. Angi, S. Muccioli, I. Szabo, L. Leanza, A meta-analysis study to infer voltage-gated K(+) channels prognostic value in different cancer types, *Antioxidants* (3) (Feb 24 2023) 12, <https://doi.org/10.3390/antiox12030573>.
- [68] M. Huber, C.U. Brehm, T.M. Gress, et al., The immune microenvironment in pancreatic cancer, *Int. J. Mol. Sci.* (19) (Oct 3 2020) 21, <https://doi.org/10.3390/ijms21197307>.
- [69] A.N. Hosen, R.A. Brekken, A. Maitra, Pancreatic cancer stroma: an update on therapeutic targeting strategies, *Nat. Rev. Gastroenterol. Hepatol.* 17 (8) (Aug 2020) 487–505, <https://doi.org/10.1038/s41575-020-0300-1>.
- [70] A.S. Bear, R.H. Vonderheide, M.H. O'Hara, Challenges and opportunities for pancreatic cancer immunotherapy, *Cancer Cell* 38 (6) (Dec 14 2020) 788–802, <https://doi.org/10.1016/j.ccell.2020.08.004>.
- [71] J.Q. Fan, M.F. Wang, H.L. Chen, D. Shang, J.K. Das, J. Song, Current advances and outlooks in immunotherapy for pancreatic ductal adenocarcinoma, *Mol. Cancer* 19 (1) (Feb 15 2020) 32, <https://doi.org/10.1186/s12943-020-01151-3>.
- [72] D. Schizas, N. Charalampakis, C. Kole, et al., Immunotherapy for Pancreatic Cancer: A 2020 Update, vol. 86, *Cancer Treat Rev.* Jun 2020, 102016, <https://doi.org/10.1016/j.ctrv.2020.102016>.